

Immunohistochemical Study of Neural Elements in Rat Alveolus Following Tooth Extraction

Thosapol Piyapattamin*, Mayuree Sarai, Pattana Haputta and Pacharapol Samneang

Faculty of Dentistry, Naresuan University, Amphor Muang, Phitsanulok 65000, Thailand.

* Corresponding author, E-mail: thosapolp@nu.ac.th

Received 6 Jan 2005
Accepted 18 May 2005

ABSTRACT: The morphology of neural elements at the alveolar sockets after tooth extraction was assessed by means of immunohistochemistry for protein gene product 9.5 (PGP 9.5) at the light microscopic level. Under general anaesthesia, maxillary right second molars of 10-week-old Wistar rats were removed. The animals were perfusion-fixed immediately after tooth extraction or 7, 30, 90, or 180 days later. Frozen sagittal cryostat sections of the decalcified maxillae were prepared and stained with the avidin-biotin complex method. Histological sections showed that alveolar sockets gradually exhibited numerous small blood vessels, osteoblasts and newly formed bone, suggesting healing processes of the post-operative wound. Throughout the experimental periods, no large PGP 9.5-immunoreactive nerve trunks were recognized. On day 7 after the tooth extraction, beaded nerve fibers were seen within the central portion and also distributed to the periphery of the healing area. They were more frequently detected on day 30, but tended to decrease in their number by day 90. Compared with those observed in the controls, Ruffini nerve endings around apical areas of the healing sockets displayed smooth and swollen contours on day 7. By day 30, no nerve endings with a morphology resembling Ruffini nerve endings were found. However, free nerve endings were noticeable in the healing areas of all animals. These results indicated that the tooth extraction caused changes in the morphology and number of nerve fibers and endings at the healing sites.

KEYWORDS: nerve fibers, nerve endings, immunohistochemistry, protein gene product 9.5.

INTRODUCTION

Mammalian teeth are attached to the jaw bone by the periodontium, consisting of cementum, gingiva, periodontal ligament (PDL), and alveolar bone. Principal fibers of PDL run between alveolar bone and cementum, causing a relationship between teeth and alveolar bone. Being a hard tissue that is composed of osteoblasts, osteocytes, osteoclasts and intercellular substances, alveolar bone serves as the foundation for a tooth and its components¹ and functions as a supportive site for tension and pressure during mastication. In addition, it protects lymph vessels, blood vessels and nerves situated in the PDL.

Innervation of oral tissues plays a major role in making regular and smooth mastication possible.^{2,3} Free nerve endings have been documented to function as nociceptors, while Ruffini nerve endings serve as mechanoreceptors. Both nerve endings can be found in all mammalian PDL,⁴⁻⁷ and their microscopic structures observable in rodents have already been confirmed by immunohistochemical methods.⁸ It has been reported that immunohistochemistry for the protein gene product 9.5 (PGP 9.5), a general marker for neural elements,⁹⁻¹¹ is useful for demonstrating nerve fibers and endings in post-natal dental structures.¹²⁻¹⁴

Dental loss results in malocclusion and affects the development of physical^{15,16} and mental¹⁷ health conditions. Furthermore, malocclusion has been reported to cause mandibular dysfunction,^{18,19} in association with an alteration of the masticatory pattern²⁰ and pain of the masticatory muscles.²¹ Clinically, natural loss of a primary tooth facilitates an eruption of its permanent successor. However, permanent tooth loss leads to a deficiency of the masticatory function at the edentulous area unless dental substitution is performed.

Although recent investigations into the morphology of neural elements in neonatal and adult rodents have been reported, those in animals following tooth extraction are scarce. Hence, it was the purpose of this study to assess the change, if any, in the morphology and the distribution of nerve fibers and endings in rats following the extraction of their maxillary second molars by using immunohistochemistry for PGP 9.5 at the light microscopic level.

MATERIALS AND METHODS

Experimental Protocol in Rats

The research protocol was approved by the Ethics Committee for Animal Experimentation, Naresuan

University, Phitsanulok, Thailand. Twenty five Wistar rats, with an age of 10 weeks old, were used in this study. They were experimentally handled according to the instructions of World Health Organization.^{22,23} The animals were kept in cages and fed with a solid diet (S.W.T. Co. Ltd., Samut Prakarn, Thailand) and water *ad libitum*. The eating and drinking behavior of the rats was monitored throughout the experimental periods. Their maxillary left second molars, as well as the areas adjacent to maxillary right first molars, were used as controls. Prior to the extraction of their maxillary right second molars, the rats were deeply anaesthetized with diethyl ether, followed by an intraperitoneal injection of sodium pentobarbital (25 mg/kg). Immediately after the extraction or 7, 30, 90 or 180 days later (n = 5 for each group), the animals were sacrificed with an overdose injection of pentobarbital and then perfused through their left ventricles with 4% paraformaldehyde in 0.1 M phosphate buffer, pH 7.4. Their maxillae were excised *en bloc* and immersed in the same fixative solution at 4°C for an additional 12 hours. The tissues were decalcified for 4 weeks at 4°C in 10% ethylene diamine tetra-acetic acid-disodium salt solution, pH 7.4.

Four decalcified maxillae from each group were washed several times in 0.01 M phosphate-buffered saline solution (PBS), pH 7.4. They were then saturated overnight at 4°C with 30% sucrose in 0.01 M PBS and embedded in O.C.T. compound (Sakura, Tokyo, Japan). Free-floating sections, 40 µm thick, were prepared serially and sagittally with a Leica CM3050 S cryostat (Leica, Nussloch, Germany), and processed for immunohistochemistry.

For histological observations, one maxilla from each group was embedded in paraffin wax. Using a rotary microtome (Leica RM2135), 4-µm thick sections were cut serially and sagittally. They were mounted on poly-L-lysine-coated glass slides (Matsunami, Osaka, Japan) and stained with hematoxylin and eosin.

Immunohistochemical Staining Protocol

The cryostat sections were processed for the avidin-biotin-complex (ABC) method, using a commercially available kit (ABC kit; Vector Laboratories, Burlingame, CA, USA). The primary antibody was the rabbit polyclonal antiserum against human PGP 9.5 (Ultraclone Co. Ltd., Cambridge, UK), the origin and characterization of which have been verified elsewhere.^{10,24,25}

In order to inactivate endogenous peroxide and non-specific immunoreactivity, all sections were pre-treated, respectively, with 0.3% H₂O₂ in absolute methanol for 30 minutes and with 2% normal goat serum (Vector Laboratories, Burlingame, CA, USA) in 0.01 M PBS containing 0.3% Triton X-100 (Sigma

Chemical, St Louis, MO, USA) for 1 hour. The sections were reacted with the primary antibody, diluted to 1:10,000 with 0.01 M PBS, for 72 hours at 4°C, followed by two consecutive incubations with biotinylated anti-rabbit IgG (Chemicon, Temecula, CA, USA) and ABC complex. At the end of each step, the sections were washed several times in 0.01 M PBS.

The immunoreactive (IR) sites were visualized with 0.02% 3,3-diaminobenzidine tetrahydrochloride and 0.01% H₂O₂ in 0.05 M Tris-HCl buffer, pH 7.6. After rinsing, the sections were attached to poly-L-lysine coated glass slides, counterstained in 1% methyl green, dehydrated in graded series of ethanol, rinsed in xylene, and mounted with Permount (Fisher Scientific, Fair Lawn, NJ, USA).

To check the specificity of the immunoreactions, the primary antibody was replaced with non-immune rabbit serum or treatment with anti-rabbit IgG or ABC was omitted.

RESULTS

No remarkable changes in the eating and drinking behavior of rats were observed after tooth extraction. During the post-extraction periods, the animals gained weight steadily (5.8 ± 1.2 g/day). Specificity controls of immunohistochemistry for PGP 9.5 showed no immunolabelled sites. However, immunohistochemistry

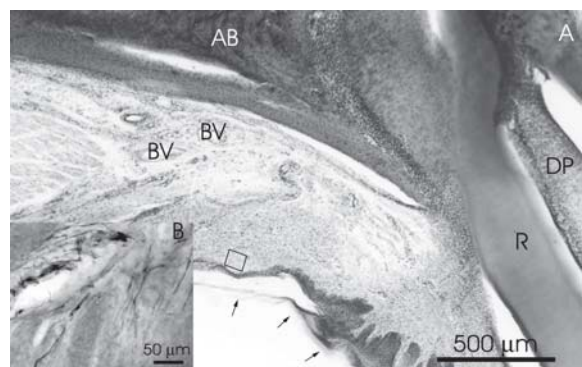


Fig 1. Light micrographs showing a sagittally cut maxilla in the area adjacent to the right first molar of a 10-week-old rat. A, H&E stained paraffin section revealing palatal mucosa which is covered with thick, keratinized (arrow), stratified squamous epithelial layers. B, Higher magnification of a cryostat section disclosing PGP 9.5-immunoreactive neural elements in the area coinciding with the boxed area in A. Note the rich innervation by fine nerve fibers within the mucosa. All nerve terminals in this area are regarded as free nerve endings, due to their sizes and the lack of any observable terminal expansions. AB: alveolar bone, BV: small blood vessel in the connective tissue layer, DP: dental pulp, R: tooth root.

of the observation area disclosed many PGP 9.5-IR elements.

Controls

Palatal mucosa located mesially to the maxillary right first molar possessed thick, orthokeratinized (and parakeratinized in some parts), and stratified squamous epithelial layers (Fig 1A). Long papillae, thick dense collagenous fibers, and moderate vascular supply with short capillary loops were also seen. Alveolar bone in this area was richly supplied with large blood vessels. PGP 9.5-IR nerve endings without any expanded terminations were found in the lamina propria (Fig 1B) and within the epithelium. Within the lamina propria, the nerve endings were usually found in the papillary region.

At maxillary left second molar, PGP 9.5-IR nerves coursed as a thick bundle from the apical foramen and alveolar socket to the PDL (Fig 2A), along a path similar to that of the adjacent blood vessels. The apical fibers entered into the PDL then either distributed within the PDL or ran downward and passed through the apical foramen to reach the dental pulp. While nerve endings ran apart from blood vessels within the PDL and sometimes terminated near the root apex, some fibers extended coronally (Fig 2B) and reached the interdental

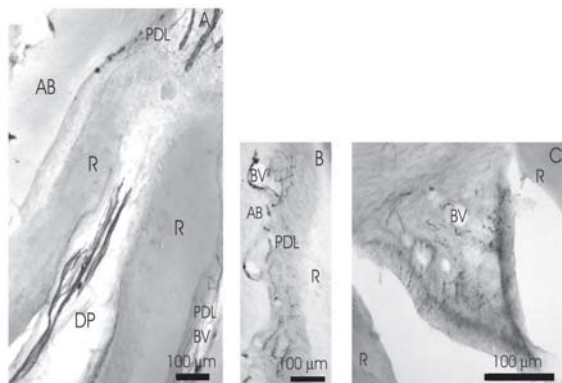


Fig 2. Light micrographs showing the distribution of PGP 9.5-immunoreactive neural elements at the maxillary left second molar of a 10-week-old rat. A, At the peripical region of mesiobuccal root (R). B, In the periodontal ligament (PDL). C, At the interdental papillary region. In Fig A, note the path of thick nerve fibers which pass through the apical foramen to reach the dental pulp (DP). Some of these show a coronal extension between R and alveolar bone (AB) by entering into and then distributing within the PDL. In Fig B, Some of the periodontal nerve endings can be observed adjacent to blood vessels (BV). The fibers running independently from the vessels are smooth in shape and seldom beaded. In Fig C, numerous thin nerve fibers are observed in the interdental papilla.

papillae (Fig 2C). Fibers running independently from blood vessels were mostly smooth in shape and seldom beaded.

In the nerve terminal-rich area of the PDL near the

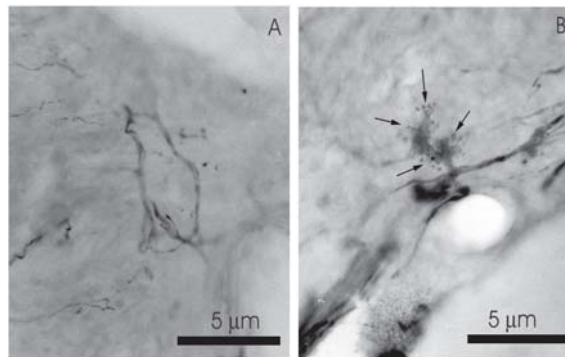


Fig 3. Light micrographs from cryostat sections showing the morphology of PGP 9.5-immunoreactive neural elements in the periodontal ligament near the root apex of the maxillary left second molar of 10-week-old rats. A, The fibers and free nerve endings observable in the periodontal ligament. Note their thinness and the seldom beaded structures. B, Nerve fibers and Ruffini nerve endings noticeable in periodontal ligament. Note their thickness and rough contour due to their numerous cytoplasmic projections (arrows). Compare the sizes and the expanded terminations between those in A and B.

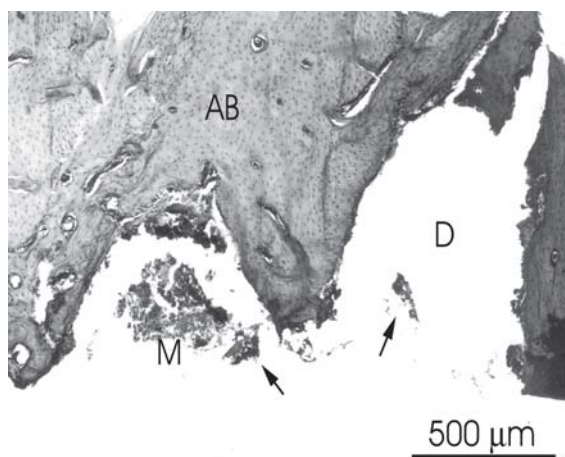


Fig 4. Light micrograph of a paraffin section on day 0 post-extraction of the rat maxillary right second molar showing an alveolar socket richly filled with blood clots (arrows) on the mesial (M) side and a socket with a small amount of blood clot on the distal (D) side. Discontinuity of the apical alveolar bone on the D side was induced during the histological process. AB: alveolar bone.

root apex, two distinct types of terminals, including free nerve endings (Fig 3A) and Ruffini nerve endings (Fig 3B), were observed. Free nerve endings and their fibers were observable in the PDL, interdental papillae, and dental pulp. Ruffini nerve endings were noticed in the PDL and interdental papillae, but not in the dental pulp. Ruffini nerve endings near the root apex tended to be located in the alveolar bone side. Their endings consisted of thick nerve fibers and expanded branches. The alveolar fibers running upward terminated among periodontal collagen fibers as free nerve endings.

Rats with an Extraction

Day 0 post-extraction – In comparison with those seen in the controls, light microscopy failed to disclose evidence of histological alterations, except for alveolar sockets filled with blood clots (Fig 4). Immunohistochemistry using PGP 9.5 revealed no changes in the neural morphology or distribution.

Day 7 post-extraction – Compared with those seen in the earlier stage, numerous small blood vessels were observed, without any other remarkable changes.

PGP 9.5-immunohistochemistry revealed minor changes on day 7. Although they were seldom found in controls, some beaded nerve fibers running independently from blood vessels were observed (Fig 5A). They were remarkable on the alveolar bone side, distributing within the central portion to the periphery of the healing area. Despite their scarceness, Ruffini nerve endings distributing around the apical area of the socket displayed a swelling shape with a smooth contour (Fig 5B), in comparison with those in the

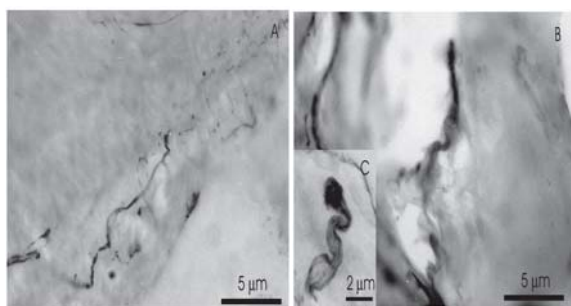


Fig 5. Light micrographs from cryostat sections showing the morphology of PGP 9.5-immunoreactive neural elements observed at the healing site on day 7 post-extraction of the rat maxillary right second molar. A, In spite of their co-existence with other nerve fibers, thin and beaded nerves run independently from the blood vessels. B, Ruffini nerve ending with a smooth contour. C, Higher magnification of another Ruffini nerve ending with a smooth and swollen contour. Compare the contour of the endings in B and C with that in Fig 3B.

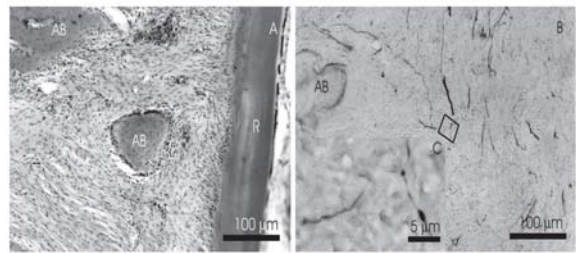


Fig 6. Light micrographs showing the healing wounds on day 30 post-extraction of a rat maxillary right second molar. A, H&E stained paraffin section revealing small islands of newly formed alveolar bone (AB) and small blood vessels throughout the site. The extraction process caused a reduction in the height of the alveolar bone crest of the adjacent tooth. The remaining interdental septum is not shown in this figure. B, Higher magnification of a cryostat section disclosing PGP 9.5-immunoreactive neural elements in the area coincident with that in A. Several thin nerve fibers distribute within and around the healing site. Beaded nerves can be more frequently observed than those in the previous stages. C, Higher magnification of the boxed area in B revealing the structure of small beaded nerves observable in this stage. R: root of maxillary right first molar.

controls (Fig 3B). Moreover, free nerve endings were recognizable within the healing sites.

Day 30 post-extraction – Healing sites showed newly formed bone with numerous osteoblasts (Fig 6A). Small islands of bone were observed at the vicinity of the newly formed bone.

Immunohistochemistry for PGP 9.5 revealed an identical distribution of beaded nerve fibers, i.e. within and around the healing sites. In comparison with those in the previous stages, beaded nerve fibers were more frequently observed (Figs 6B, 6C). Free nerve endings found in and around the healing area resembled those on day 7. However, no Ruffini nerve endings were detectable at this stage.

Day 90 and day 180 post-extraction – Small blood vessels were frequently recognized at the healing sites on both day 90 and day 180. A deposit of newly formed bone and new capillaries were also observed (Figs 7A, 7B). Fine arrangement of connective tissue fibers within the healing site was also recognized (Fig 7B).

On day 90 and day 180 post-extraction, the incidence of beaded fibers decreased and the path of the nerves became less undulated. Only nerve terminals with a structure similar to free nerve endings were observed, not Ruffini nerve endings.

DISCUSSION

The results in this study provide evidence of changes

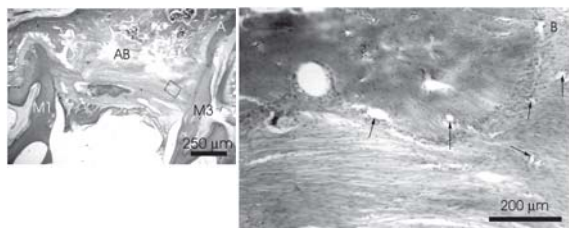


Fig 7. Light micrographs showing the healing wounds on day 90 post-extraction of a rat maxillary right second molar. A, H&E stained paraffin section revealing good wound healing condition with newly formed alveolar bone (AB). B, Higher magnification showing several blood vessels (arrows) and an arrangement of the connective tissue fibers. M1: first molar, M3: third molar.

in nerve fibers and endings occurring at the healing sites of rat molar regions.

Due to the fact that silver salts and the recently described neurofilament protein (NFP) and neuropeptides (NP) fail to disclose all nerves,¹¹ PGP 9.5 was selected as a marker in our study. Anti-NFP and anti-NP are unsuitable for the detection of the thin C-fibers²⁶ and thick fibers,²⁷ respectively. However, the anti-PGP 9.5 is a cytoplasmic protein in central and peripheral neurones,^{10,24,25} thus allowing it to stain all types of neurones. The neural elements observed in this study coincide with the previous findings.²⁸

Beaded PGP 9.5-IR nerve fibers with irregular paths were recognized post-extraction from day 7 onward. Generally, beaded morphology is regarded as degenerated, regenerating, or NP-containing nerve fibers.^{13,14,29,30} In comparison with previous investigations in the inflammatory and healing processes in carious teeth³¹ and in dental pulp tissues,^{32,33} our data correlated well with theirs in that beaded nerves can be more frequently found while the processes are progressing. Beaded nerves contain various types of NP.³⁴ They are involved in a variety of biological mechanisms, including neurogenic inflammation,³⁵ modulation of immune cell functions,³⁶ regulation of endothelial cell growth,³⁷ and neurotransmission of nociceptive input.³⁸ A significant increase in pulpal neural density with caries progression was disclosed by one investigation.³¹ Nevertheless, no correlation was concluded between reported pain experienced and overall neural density. It is considered unlikely that NP directly sensitizes nociceptive afferents. However, it may exert an indirect effect via its numerous vasodilatory and pro-inflammatory interactions.³⁹ Hence, peripheral sensitization is likely to contribute

to the hyperalgesia which is clinically associated with the commencement of healing processes.

Mason and Holland⁴⁰ used a model of extraction similar to ours; however, they performed silver staining histology of single rooted mandibular canines, while we analyzed all roots of maxillary second molars using an immunohistochemical method. In their study, silver stained-nerve fibers increased in number from one month. Nevertheless, our study revealed an increase of beaded nerve fibers much earlier on day 7 post-extraction. They also stated that a number of silver-stained structures contained nerve trunks three months after tooth extraction. In spite of our careful investigation, we failed to detect such large nerve trunks in any immunohistochemically-treated sections. The discrepancies between their findings and ours remain to be clarified, yet they may be attributable to the different observation areas. They confined the area to the canine that had only one root, whereas we carried out a global observation on all roots of the second molar. The increased prominence of beaded nerves in experimental rats from day 7 to day 90 and their gradual decrease seemed to coincide with new bone formation. The increased number of beaded nerve endings, which are thought to be nociceptors, found in the areas filled with bone may be associated with the pain perception at the healing sites by patients after tooth extraction.

At the healing wounds, Ruffini nerve endings possessing a swollen and smooth contour which might be due to the loss of their cytoplasmic projections, were found on day 7 after tooth extraction and disappeared by day 90. According to recent reports,^{13,14} the post-natal morphology of rodent periodontal nerves undergoes a complex developmental process and functional stimuli contribute to their final differentiation. The post-natal development of Ruffini nerve endings verifies a close relationship between their configuration and functional forces from occlusion. However, Ruffini nerve endings observed in aged rodents⁴¹ and in hypofunctional periapex⁴² were reported to possess a club-shaped morphology with few, if any, microprojections. At the electron microscopic level, they contained large vacuoles and much less mitochondria. Taken together, this illustrated that the Ruffini nerve endings recognized at the healing sites of alveolar sockets underwent a degenerating process.

Several types of normal oral flora found in rats are documented, such as *Coliform*, *Corynebacterium*, *Paracolon bacilli*, *Staphylococci* and *Streptococci*.⁴³ Despite the environment within the oral cavity and the use of no pre- or post-operative antibiotics, the experimental animals survived to the dates of fixation. Moreover, the sites of extraction showed good healing processes with innervation, as shown in our results. Alterations in the morphology and distribution of nerve fibers and

endings cannot be absolutely extrapolated to the physiological changes in nociception or mechanoreception. Nonetheless, the possibility that the increase in the number of beaded nerves and the decrease in the number of Ruffini endings might affect nociception and/or mechanoreception in patients after tooth extraction, if similar changes also occur in humans, cannot be excluded.

The present results revealed that tooth extraction leads to alterations in the morphology and number of neural elements within the healing sites. This would reflect the innervation of healing alveolar bone occurring soon after the clinical process. An animal experiment accommodating the nerve regeneration process beyond the 180-day period examined here remains to be investigated.

ACKNOWLEDGEMENTS

The authors are grateful to Mr. Sunya Chiamsuk for his technical supports. This work was partially supported by the research grant of the Faculty of Dentistry, Naresuan University.

REFERENCES

- Bhaskar SN (1986) Maxilla and mandible (alveolar process). In: *Orban's Oral Histology and Embryology, 11th ed*, pp 239-59. Mosby-Year Book, St Louis, MO.
- Matthews B (1975) Mastication. In: *Applied Physiology of the Mouth, 1st ed* (Edited by Lavelle CLB), pp 199-242. John Wright and Sons, Bristol, UK.
- Linden RWA (1990) Periodontal mechanoreceptors and their function. In: *Neurophysiology of the Teeth and Jaws, 1st ed* (Edited by Taylor A), pp 52-88. Macmillan Press, London, UK.
- Maeda T, Kannari K, Sato O and Iwanaga T (1990) Nerve terminals in human periodontal ligament as demonstrated by immunohistochemistry for neurofilament protein (NFP) and S-100 protein. *Arch Histol Cytol* **53**, 259-65.
- Cash RM and Linden RWA (1982) The distribution of mechanoreceptors in the periodontal ligament of the mandibular canine tooth of the cat. *J Physiol* **330**, 439-47.
- Sato O, Maeda T, Iwanaga T and Kobayashi S (1989) Innervation of the incisors and PDL in several rodents: an immunohistochemical study of neurofilament protein and glia-specific S-100 protein. *Acta Anat* **134**, 94-9.
- Linden RWA, Millar BJ and Scott BJJ (1995) The innervation of the periodontal ligament. In: *The Periodontal Ligament in Health and Disease, 2nd ed* (Edited by Berkovitz B, Moxham BJ and Newman N), pp 133-59. Mosby-Wolfe, London.
- Sato O (1998) Innervation of periodontal ligament and dental pulp in the rat incisor: an immunohistochemical investigation of neurofilament protein and glia-specific S-100 protein. *Cell Tissue Res* **251**, 13-21.
- Schmechel D, Marangos PJ and Brightman M (1978) Neurone-specific enolase is a molecular marker for peripheral and central neuroendocrine cell. *Nature* **276**, 834-6.
- Thompson RJ, Doran JF, Jackson P, Dhillon AP and Rode J (1983) PGP 9.5: a new marker for vertebrate neurons and neuroendocrine cells. *Brain Res* **278**, 224-8.
- Ramieri G, Anselmetti GC, Baracchi F, Panzica GC, Viglietti-Panzica C, Modica R and Polak JM (1990) The innervation of human teeth and gingival epithelium as revealed by means of an antiserum for protein gene product 9.5. *Am J Anat* **189**, 146-54.
- Fristad I, Heyeraas KJ and Kvinnsland I (1994) Nerve fibres and cells immunoreactive to neurochemical markers in developing rat molars and supporting tissues. *Arch Oral Biol* **39**, 633-46.
- Nakakura-Ohshima K, Maeda T, Sato O and Takano Y (1993) Postnatal development of periodontal innervation in rat incisors: an immunohistochemical study using protein gene product 9.5 antibody. *Arch Histol Cytol* **56**, 385-98.
- Nakakura-Ohshima K, Maeda T, Ohshima H, Noda T and Takano Y (1995) Postnatal development of periodontal Ruffini endings in rat incisors: an immunoelectron microscopic study using protein gene product 9.5 antibody. *J Comp Neurol* **362**, 551-64.
- Jackson-Herrerias G, Flores-Vazquez LE and Marquez-Avila CS (1991) Phoniatic changes in children aged 3 to 5 years after premature loss of upper incisors. *Bol Med Hosp Infant Mex* **48**, 96-100.
- Kim J and Nielsen IL (2000) A longitudinal study of condylar growth and mandibular rotation in untreated subjects with Class II malocclusion. *Angle Orthod* **72**, 105-11.
- Judd PL and Casas MJ (1995) Psychosocial perceptions of premature tooth loss in children. *Ont Dent* **72**, 16-23.
- Mohlin B and Kopp S (1978) A clinical study of the relationship between malocclusions, occlusal interferences and mandibular pain and dysfunction. *Swed Dent J* **2**, 105-12.
- Egermark-Eriksson I, Ingervall B and Carlsson GE (1983) The dependence of mandibular dysfunction in children on functional and morphologic occlusion. *Am J Orthod* **83**, 187-94.
- Kitamura E, Takashima F, Miyauchi S and Maruyama T (1987) The effect of anterior crossbite on stomatognathic function. *Nippon Hotetsu Shika Gakkai Zasshi* **31**, 1216-26.
- Proffit WR (2000) The etiology of orthodontics problems. In: *Contemporary Orthodontics, 3rd ed* (Edited by Proffit WR and Fields HW), pp 113-144. C.V. Mosby, St Louis, MO.
- ECBA (1989) Competence of biologists for experiments on animals. In: *Report of the Workshop organised by the European Communities Biologists Association at Amsterdam, The Netherlands, March 7-9, 1988* (Edited by van Emden HM, de Cock Buning T and Lopes da Silva FH), ECBA publication, Geneva.
- ECBA (1989) Animal experimentation: legislation and education on animals. In: *Proceedings of the EC Workshop in Bilthoven, The Netherlands, May 22-24, 1989* (Edited by van Zutphen LFM, Rozemond H and Beynen AC), Veterinary Public Health Inspectorate, and Utrecht: Department of Laboratory Animal Science, Geneva.
- Doran JF, Jackson P, Kynoch PA and Thompson RJ (1983) Isolation of PGP 9.5, a new human neuron specific protein detected by high-resolution two-dimensional electrophoresis. *J Neurochem* **40**, 1542-7.
- Gulbenkian S, Wharton J and Polak JM (1987) The visualization of cardiovascular innervation in the guinea pig using antiserum to protein gene product 9.5 (PGP 9.5). *J Auton Nerv Syst* **18**, 235-47.
- Maeda T and Sato O (1992) Sensory receptors in the periodontal ligament demonstrated by immunohistochemistry for nervous-specific proteins and

- electron microscopy. In: *Biological Mechanisms of Tooth Movement and Craniofacial Adaptation*, 1st ed (Edited by Davidovitch Z and Mah J), pp 485-96. Ebsco Media, Birmingham, AL.
27. Kato J, Tanne K and Ichikawa H (1992) Distribution of calcitonin gene-related peptide and substance P-immunoreactive nerve fibers and their correlation in the periodontal ligament of the mouse incisor. *Acta Anat* **145**, 101-5.
 28. Schroeder HE (1986) Development, structure, and function of periodontal tissues. In: *Handbook of Microscopic Anatomy*, 1st ed (Edited by Oksche A and Vollrath L), pp 170-233. Springer-Verlag, Berlin, Germany.
 29. Piyapattamin T, Takano Y, Eto K and Soma K (1999) Morphological changes in periodontal mechanoreceptors of mouse maxillary incisors after the experimental induction of anterior crossbite: a light and electron microscopic observation using immunohistochemistry for PGP 9.5. *Eur J Orthod* **21**, 15-29.
 30. Wakisaka S, Youn SH, Maeda T and Kurisu K (1996) Neuropeptide Y-like immunoreactive primary afferents in the periodontal tissues following dental injury in the rat. *Regul Pept* **63**, 163-9.
 31. Rodd HD and Boissonade FM (2000) Substance P expression in human tooth pulp in relation to caries and pain experience. *Eur J Oral Sci* **108**, 467-74.
 32. Swift ML and Byers MR (1992) Effect of aging on responses of nerve fibres to pulpal inflammation in rat molars analysed by quantitative immunocytochemistry. *Arch Oral Biol* **11**, 901-12.
 33. Hong D, Byers MR and Oswald RJ (1993) Dexamethasone treatment reduces sensory neuropeptides and nerve sprouting reactions in injured teeth. *Pain* **55**, 171-81.
 34. Wakisaka S, Ichikawa H, Nishimoto T, Matsuo S, Yamamoto K, Nakata T, Akai M (1984) Substance P-like immunoreactivity in the pulp-dentine zone of human molar teeth demonstrated by indirect immunofluorescence. *Arch Oral Biol* **29**, 73-5.
 35. Lembeck F and Holzer P (1979) Substance P as neurogenic mediator of antidromic vasodilation and neurogenic plasma extravasation. *Arch Pharmacol* **310**, 175-83.
 36. McGillis JP, Organist ML and Payan DG (1987) Substance P and immunoregulation. *Fed Proc* **46**, 196-9.
 37. Nilsson J, von Euler AM and Dalsgaard C (1985) Stimulation of connective tissue cell growth by substance P and substance K. *Nature* **315**, 61-3.
 38. Fleetwood-Walker SM (1995) Nonopoid mediators and modulators of nociceptive processing in the spinal dorsal horn as targets for novel analgesis. *Pain Rev* **2**, 153-73.
 39. Basbaum AI (1999) Distinct neurochemical features of acute and persistent pain. *Proc Natl Acad Sci USA* **96**, 7739-43.
 40. Mason AG and Holland GR (1993) The reinnervation of healing extraction sockets in the ferret. *J Dent Res* **72**, 1215-21.
 41. Piyapattamin T and Limwongse V (2002) Morphological changes of Ruffini nerve endings in the periodontal ligament of aged mice. *ScienceAsia* **28**, 339-44.
 42. Muramoto T, Takano Y and Soma K (2000) Time-related changes in periodontal mechanoreceptors in rat molars after the loss of occlusal stimuli. *Arch Histol Cytol* **63**, 369-80.
 43. Keele BB (1977) The oral environment in experimental animals: the microflora. In: *Animal Models in Dental Research*, 1st ed (Edited by Navia JM), pp 197-224. The University of Alabama Press, AL.